

Chapters 1 Preliminary Concepts & 2 Fundamental Equations of Compressible Viscous Flow

Historical Outline

Faces of Fluid Mechanics



Archimedes
(287-212 BC)

Newton
(1642-1727)

Leibniz
(1646-1716)

Bernoulli
(1667-1748)



Euler
(1707-1783)

Navier
(1785-1836)

Stokes
(1819-1903)

Reynolds
(1842-1912)



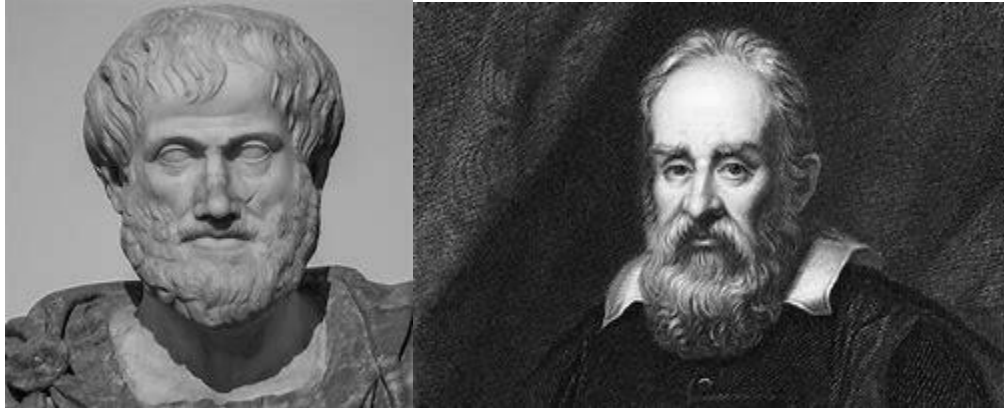
Prandtl
(1875-1953)

Taylor
(1886-1975)

Kolmogorov
(1903-1987)

Summit: fastest in world
Speed: 148.6 petaFLOPS
Cores: 2,414,592
IBM
Oak Ridge National Laboratory,
USA

21st Century Scientific Method Paradigm



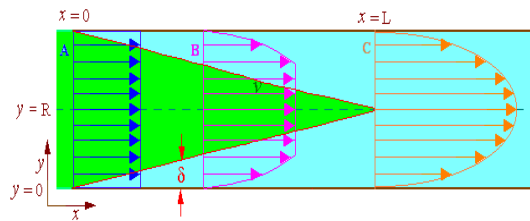
Logic

Observation/Experimentation

Future: Simulation based design based, which combines logic/computers, experiments/validation and data driven methods for scientific engineering

Some Examples of Viscous Flow Phenomena

Analytical Fluid Mechanics (AFD)



δ = Boundary layer thickness
 R = Radius of pipe
 L = Transition length
 v = Velocity

Potential flow regime

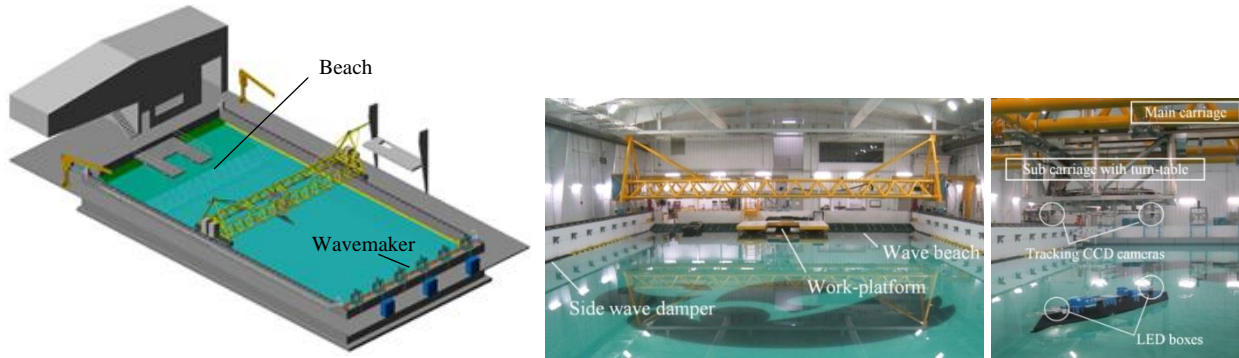
Boundary layer flow

Development of boundary-layer flow in pipe

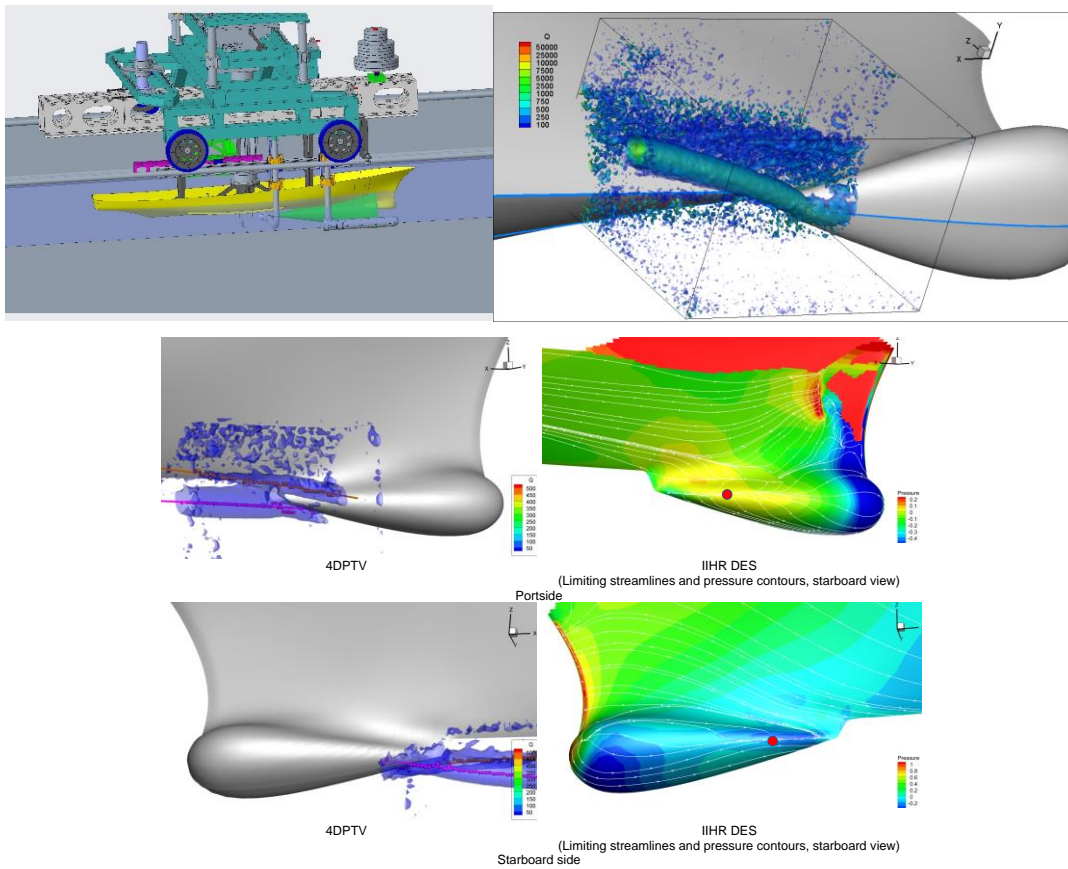
$$\nabla \cdot \mathbf{U} = 0$$

$$\frac{D\mathbf{U}}{Dt} = -\nabla p + \frac{1}{Re} \nabla^2 \mathbf{U} + \nabla \cdot \overline{u_i u_j}$$

Experimental Fluid Mechanics (EFD)



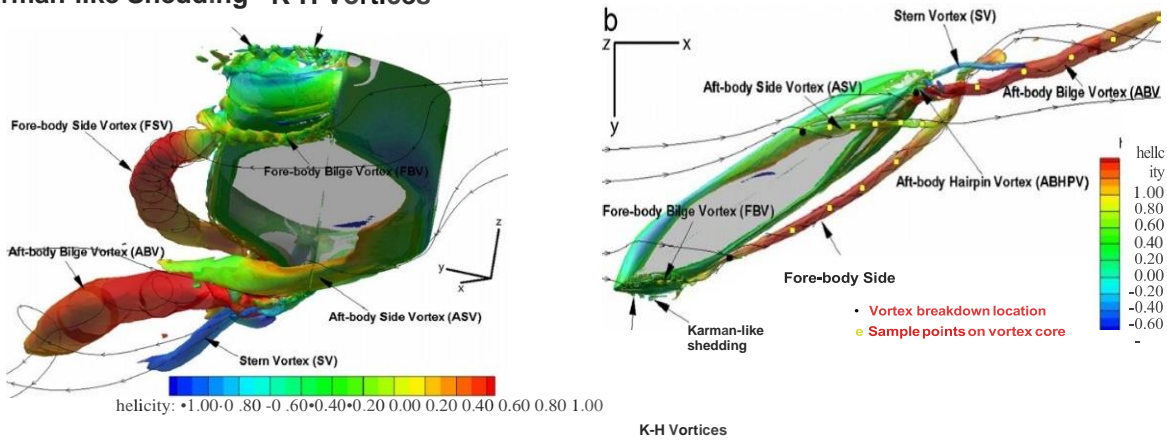
IIHR wave basin



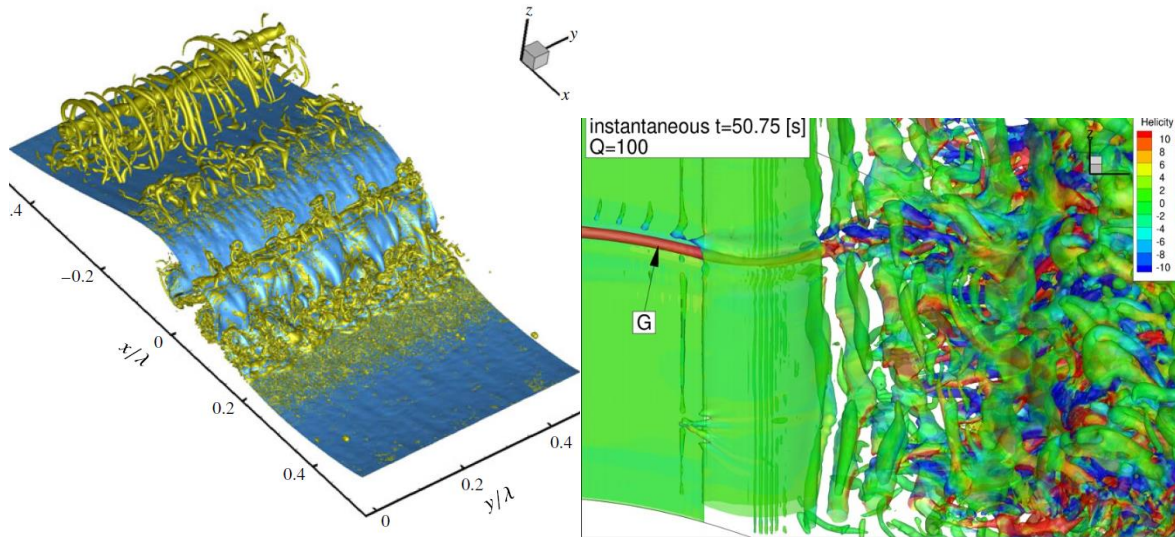
Local Flow 4DPTV Measurement System in IIHR Towing Tank

Computational Fluids Mechanics (CFD)

Karman-like Shedding K-H Vortices

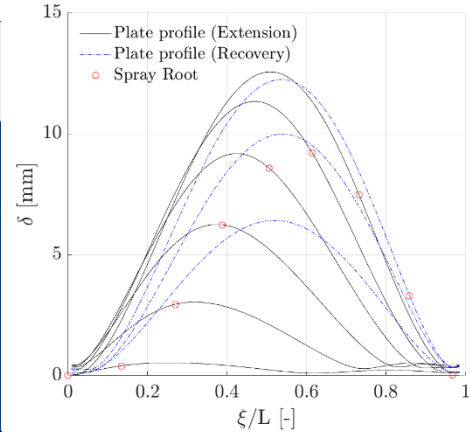
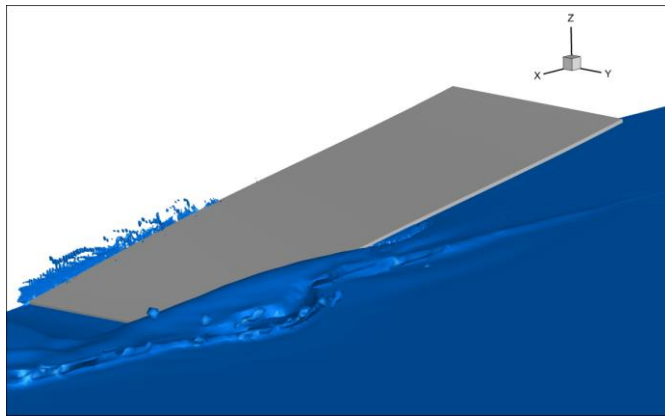


Vortex system of KVLCC2 (iso surface of $Q=200$ colored by helicity) at $\beta=30^\circ$: (a) bow view and (b) bottom view.



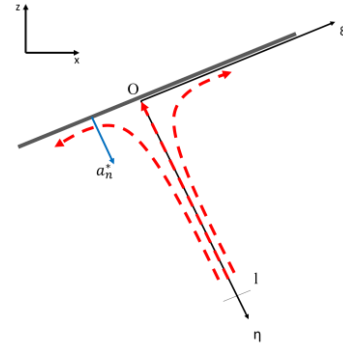
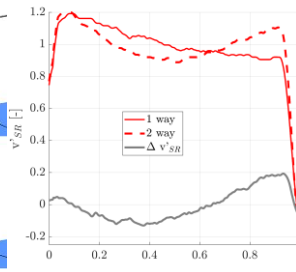
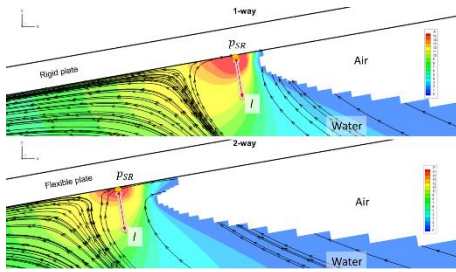
CFDShip-Iowa DNS of breaking wave and bulge-scare air-water interface instability

CFDShip-Iowa & ANSYS Fluid Structure Interaction (FSI)



Stagnation Flow Model: Extended Bernoulli Equation Analysis

$$p_{SR} = \rho \left(\frac{\Delta v_n^2}{2} - a_n^* l \right) = p_{SR}|_{2way} - p_{SR}|_{1way} \propto \rho \left(\frac{\Delta v_n^2}{2} - l a_n^* \right)$$



FSI Conservation of energy analysis

$$-\frac{\delta W}{dt} = \frac{dE}{dt} = \frac{\partial}{\partial t} \iiint_{V(t)} e \rho dV + \iint_{S(t)} e \rho (\mathbf{u} \cdot \hat{\mathbf{n}}) dS$$

$$e = k_e + p_{e\varepsilon} + p_{eg}$$

Kinetic energy and elastic and gravitation potential energies

CFDSHIP-IOWA & ANSYS multi-disciplinary optimization (MDO)

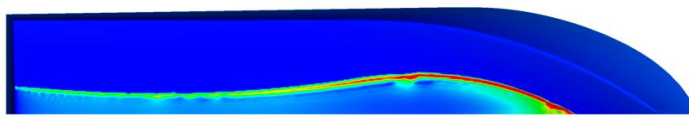


(a)

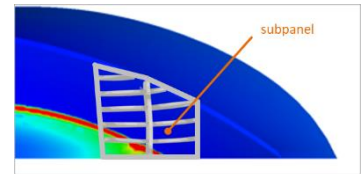
(b)

(c)

Figure 2: GPPH grillage traditional design: location (a), experimental (b), and FE model (c).

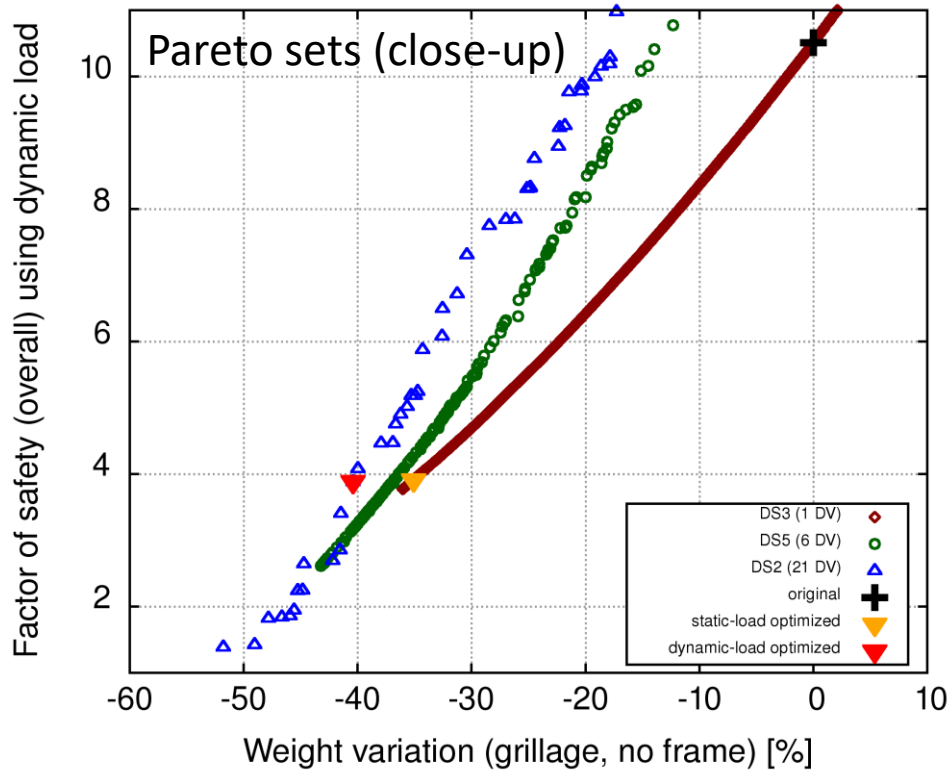


(a)



(b)

Figure 3: Evaluation of hydrodynamic loads by CFD (bottom view).



1-2 Some examples of viscous-flow phenomena (continued)

Overview

types of flows:

incompressible: $\rho = \text{constant}$ $\nabla \cdot \underline{v} = 0$
 Compressible: $\rho \neq \text{constant}$ $\rho_t + \nabla \cdot \rho \underline{v} = 0$

inviscid ($\mu = 0$), incompressible flow

ca. 1750 $\rho \frac{D\underline{v}}{Dt} = \rho \underline{g} - \nabla p$ Euler equation $\frac{D}{Dt} = \frac{\partial}{\partial t} + \underline{v} \cdot \nabla$
 inertia = (gravitational) body force - (pressure) surface force

ideal flow ($\mu = 0$, $\rho = \text{constant}$, $\underline{\omega} = \nabla \times \underline{v} = 0$)

$\underline{v} = \nabla \phi$
 $\nabla \cdot \nabla \phi = 0$
 $\nabla^2 \phi = 0$ Laplace equation

ca. 1750 $\rho \frac{\partial \phi}{\partial t} + \rho + \frac{1}{2} \rho \nabla \phi \cdot \nabla \phi + \rho g z = \text{constant}$ Bernoulli equation

viscous, compressible flow

ca. 1850 $\rho \frac{D\underline{v}}{Dt} = \rho \underline{g} + \nabla \cdot \underline{\tau}'_{ij} - \nabla p$ Navier-Stokes equations
 $\rho \frac{Dh}{Dt} = \frac{\partial h}{\partial t} + \nabla \cdot (\lambda \nabla T) + \underline{\tau}'_{ij} \frac{\partial u_i}{\partial x_j}$ energy equation

$$\underline{\tau}'_{ij} = \mu \left(\frac{\partial u_i}{\partial x_j} + \frac{\partial u_j}{\partial x_i} \right) + \delta_{ij} \lambda \nabla \cdot \underline{v} \quad (\lambda = -\frac{2}{3} \mu)$$

Analysis techniques:

Analytical: mathematical solutions
restricted to simplified flows and/or equations (CFD)

Computational Fluid Dynamics: computed solutions
current approach and future approach for $\begin{matrix} \text{BD} \\ \text{EFD} \end{matrix}$

Experimental Fluid Dynamics: measured solutions
basis for design and theory at req. for CFD validation

Uncertainty analysis:

EFD: ASME JFE (1991)

$$U_{\text{result}} = [B^2 + P^2]^{1/2} \quad \text{RSS}$$

bias precision

CFD: ASME JFE (1993)

$$U_{\text{result}} = [M^2 + W^2]^{1/2} \quad \text{RSS}$$

mostly numerical
eq. + physics num. sol. mathematical equations

determination of model error req.
validation is comparison with EFD

determination of numerical error req.
verification is assessment of stability
and grid convergence, effects of
artificial viscosity, at order of accuracy

QR
BL
NS
RANS
LES → DES
DNS

local
pivot
between
LOV
VIV
4DPIV

Modern V&V and UQ Methods

Coleman, H.W. and Stern, F., “[Uncertainties and CFD Code Validation](#),” ASME J. Fluids Eng., Vol. 119, December 1997, pp. 795 – 803

Stern, F., Wilson, R.V., Coleman, H., and Paterson, E., “[Comprehensive Approach to Verification and Validation of CFD Simulations-Part 1: Methodology and procedures](#),” ASME J. Fluids Eng., Vol. 123, Issue 4, December 2001

Xing, T. and Stern, F., “[Factors of Safety for Richardson Extrapolation](#),” ASME J. Fluids Eng., Vol. 132, June 2010

Diez M., Broglia R., Durante D., Olivieri A., Campana E.F., Stern F., “[Validation of Uncertainty Quantification Methods for High-Fidelity CFD of Ship Response in Irregular Waves](#),” ASME Journal of Verification, Validation and Uncertainty Quantification, JUNE 2018, Vol. 3.

Multiple EFD and CFD Methods

Stern, F., Olivieri, A., Shao, J., Longo, J., and Ratcliffe, T., “[Statistical Approach for Estimating Intervals of Certification or Biases of Facilities or Measurement Systems Including Uncertainties](#),” ASME J. Fluids Eng., Vol. 127, No. 2, May 2005, pp. 604 – 610

Stern, F., Diez, M., Sadat-Hosseini, H., Yoon, H., Quadvlieg, F., [Statistical Approach for CFD State-of-the-Art Assessment: N-Version Verification and Validation](#), ASME Journal of Verification, Validation and Uncertainty Quantification, 2017, Vol. 2.

Simulation Based Design

CFD + EFD + Optimization + V&V and UQ are new paradigm for development for simulation-based design, which is rapidly being augmented by including FSI and MDO capabilities with addition of data driven/machine learning and other physics of interest on the near horizon

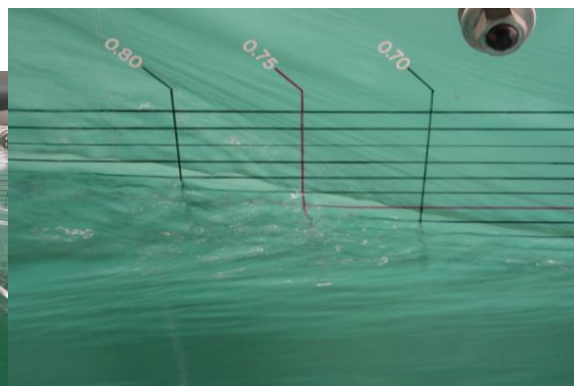
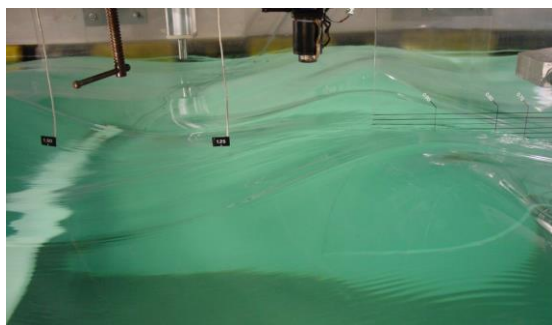
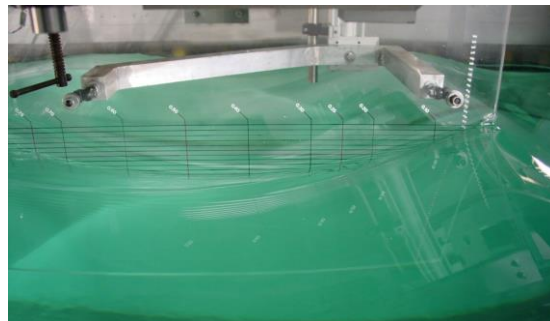
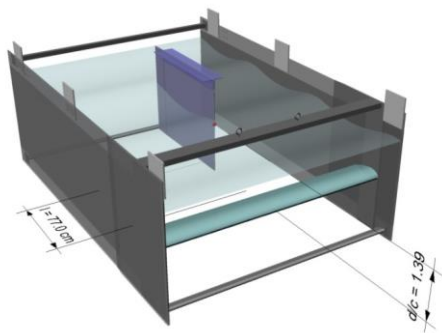
This Course:

Mostly analytical solutions for simple flows of exact (linear, 2D) and approximate (boundary layer) equations. These solutions are very important for physical understanding and represent building block for “real world” industrial applications.

IIHR Ship Hydrodynamics Selected Viscous Flow Examples

Wave-Induced Separation

Stern, F., Choi, J.E., and Hwang, W.S., “[Effects of Waves on the Wake of a Surface-Piercing Flat Plate: Experiment and Theory](#),” *Journal of Ship Research*, Vol. 37, No. 2, June 1993, pp. 102 – 118



Xing, T., Kandasamy, M., and Stern, F., “[Unsteady Free-Surface Wave-Induced Separation: Analysis of Turbulent Structures Using Detached Eddy Simulation and Single-Phase Level Set](#),” *Journal of Turbulence*, Vol. 8, No. 44, 2007, pp. 1 – 35

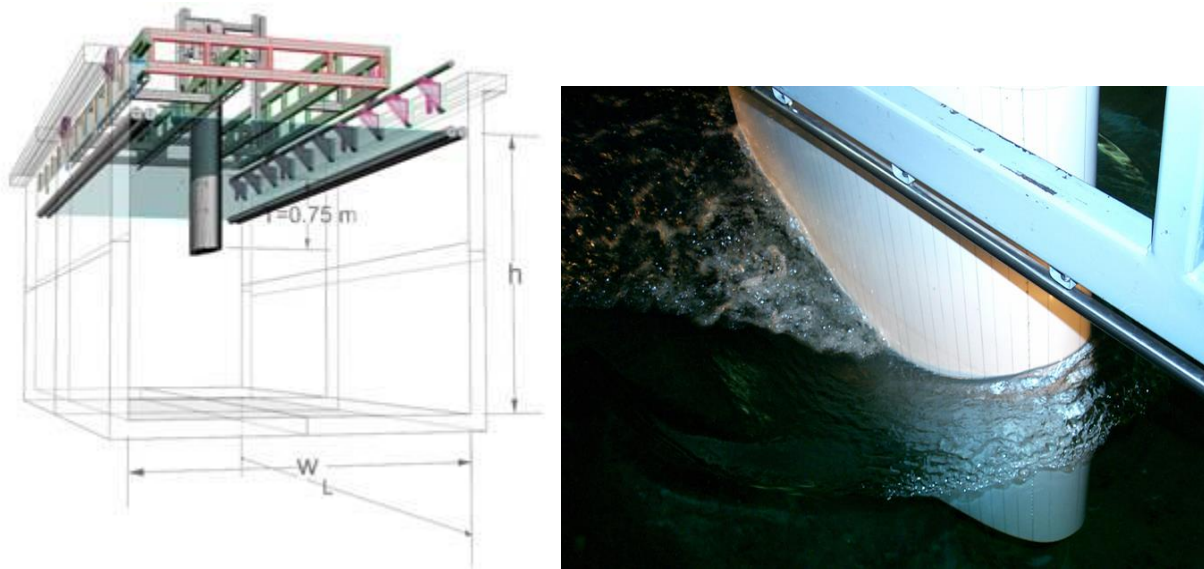


Figure 1. Photo of the surface-piercing NACA0024 hydrofoil at $Fr=0.37$ (EFD).

Wave Breaking & Air-Water Interface Instabilities

Kang, DH, Ghosh, S., Reins, G., Koo, B., Wang, Z., Stern, F., “[Impulsive Plunging Wave Breaking Downstream of a Bump in a Shallow Water Flume – Part I: Experimental Observations](#),” *Journal of Fluids and Structures*, invited for special issue for FEDSM2010-ICNMM2010, Vol. 32, July 2012, pp. 104 – 120. [Movie](#)

Koo, B., Wang, Z., Yang, J., Stern, F., “[Impulsive Plunging Wave Breaking Downstream of a Bump in a Shallow Water Flume – Part II: Numerical Simulations](#),” *Journal of Fluids and Structures*, invited for special issue for FEDSM2010-ICNMM2010, Vol. 32, July 2012, pp.121 – 134.

Wang, Z., Yang, J., and Stern, F., “[High-fidelity simulations of bubble, droplet, and spray formation in breaking waves](#),” *JFM*, 2016, vol. 792, pp. 307-327. [Movie](#)

Timur Kent Dogan, Zhaoyuan Wang and Frederick Stern, “[Experimental and Numerical Study of Air-Water Interface Instabilities with Machine Learning for Experimental Data Analysis](#),” 33rd Symposium on Naval Hydrodynamics Osaka, Japan, 31 May-5 June 2020. [Movies: EFD Instability, SL1 and SL2; DNS 1, 2 & 3](#)

Unsteady Separation

Xing, T. Bhushan, S., and Stern, F. “[DES for a Tanker at Drift Angles with Analogy to Delta Wings](#),” *Ocean Engineering*, Volume 55, December 2012, pp. 23 – 43.

Bhushan, S., Yoon, H, Stern, F, Guilmineau, E., Visonneau, M., Toxopeus, S., Simonsen, C., Aram, S., Kim, S.-E. and Grigoropoulos, G., “[Assessment of CFD for Surface Combatant 5415 at Straight Ahead and Static Drift \$\beta=20^\circ\$](#) ,” ASME JFE, MAY 2019, Vol. 141.

S.M. Yeon, J. Yang, F. Stern, [Large-Eddy Simulation of the Flow past a Circular Cylinder at Sub- to Super-Critical Reynolds Numbers](#), Applied Ocean Research, 59 (2016) 687-708.

Frederick Stern, “[Effects of Sway Motion on Smooth-Surface Vortex Separation Onset and Progression: Surface Combatant and Surface-Piercing Truncated Cylinder](#),” AVT-307: Research Symposium on Separated Flow: Prediction, Measurement and Assessment for Air and Sea Vehicles, Trondheim, Norway, 07-09 October 2019.

Yugo Sanada, Sungtek Park, Dong Hwan Kim, Zhaoyuan Wang, Hironori Yasukawa, and Frederick Stern, “[Experimental and CFD Study of KCS Hull-Propeller-Rudder Interaction for Self-Propulsion and Port and Starboard Turning Circles](#),” submitted Applied Ocean Research, January 2021. [Movie 1 & 2](#)

Turbulence Anisotropy

Longo, J., Huang, H.P., and Stern, F., “[Solid-Fluid Juncture Boundary Layer and Wake](#),” *Experiments in Fluids*, Vol. 25, No. 4, September 1998, pp. 283 – 297

Frederick Stern, “[Integrated High-Fidelity Validation Experiments and LES for a Surface-Piercing Truncated Cylinder for Sub- and Critical Reynolds and Froude Numbers](#),” AVT-246: Progress and Challenges in Validation Testing for CFD, Avila, Spain, 26-28 September 2016. [Movie \(1, 2, 3, 4\)](#)

Frederick Stern, “[Effects of Sway Motion on Smooth-Surface Vortex Separation Onset and Progression: Surface Combatant and Surface-Piercing Truncated Cylinder](#),” AVT-307: Research Symposium on Separated Flow: Prediction, Measurement and Assessment for Air and Sea Vehicles, Trondheim, Norway, 07-09 October 2019. [Movie \(1, 2, 3, 4\)](#)

Examples

(a) Flow past a circular cylinder

Inviscid-flow solution: analytical

$$\underline{v} = \nabla \phi = u_r \hat{e}_r + u_\theta \hat{e}_\theta$$

↖ velocity potential ($\nabla^2 \phi = 0$, etc.)

$$\phi = U \cos \theta (r + R^2/r) = \text{uniform stream} + \text{dipole}$$

$$u_r = U \cos \theta (1 - R^2/r^2)$$

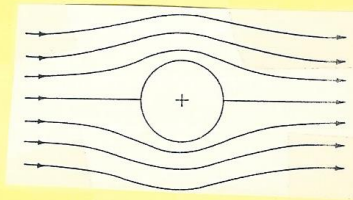
$$u_\theta = -U \sin \theta (1 + R^2/r^2)$$

on $r = R$:

$$u_r = 0$$

$$u_\theta = -2U \sin \theta$$

$$C_p = 1 - 4 \sin^2 \theta$$



$$Re = \rho U D / \mu$$

$$= U D / \nu$$

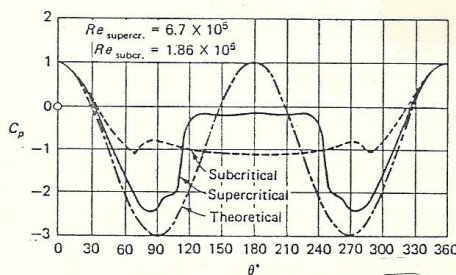
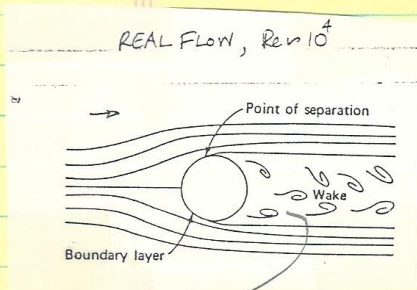


FIGURE 1-3 Comparison of perfect-fluid theory and an experiment for the pressure distribution on a cylinder. [After Flachsbarth (1932).]

Viscous-flow solution: EFD and CFD,
 although CFD restricted for low
 Re. (laminar flow)



inter sheet

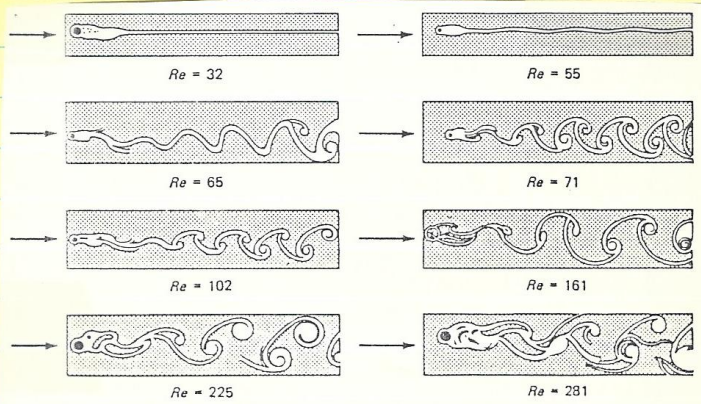


FIGURE 1-5
 The effect of Reynolds number on the flow past a cylinder. [After Homann (1936).]

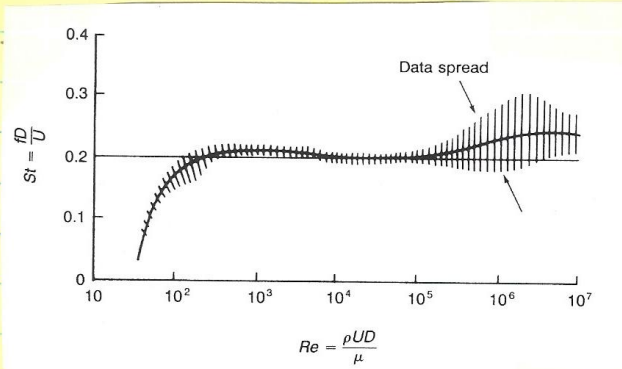
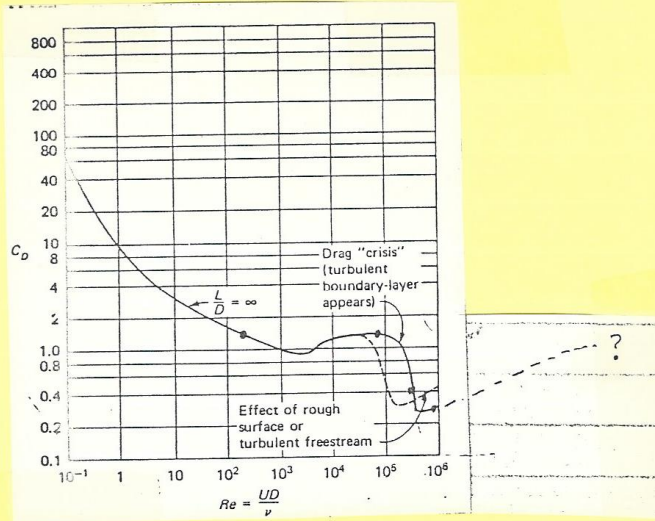


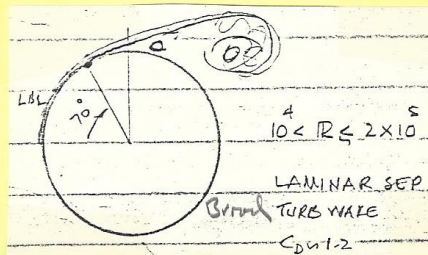
FIGURE 1-8
 Measured Strouhal number for vortex shedding frequency behind a circular cylinder.

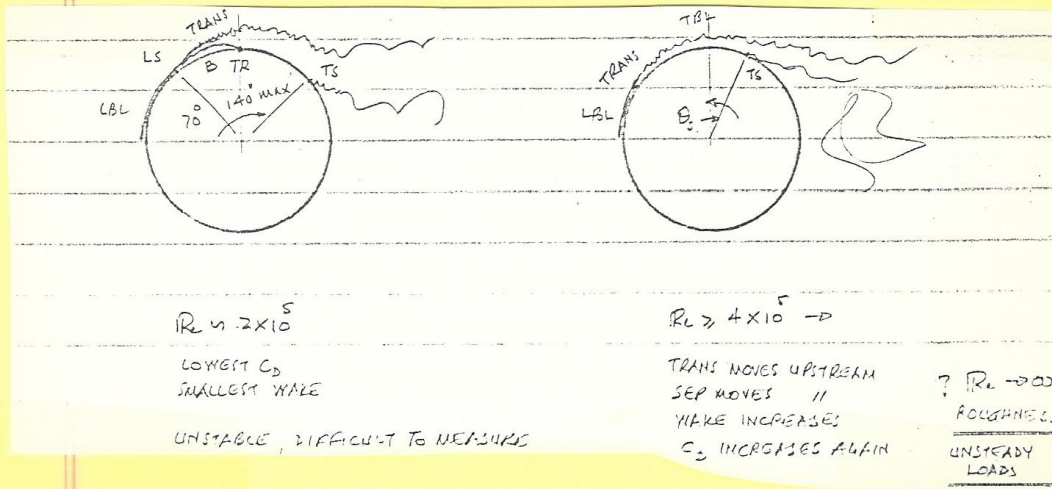
variation
is several
orders of
magnitude

$$C_D = \frac{D}{\frac{1}{2} \rho U^2 A}$$



- * at low Re , flow is purely viscous (Stokes flow)
at C_D is large (i.e. $D/A \gg \frac{1}{2} \rho U^2$)
↖ freestream dynamic pressure
- * at medium and high Re , $D/A \approx \frac{1}{2} \rho U^2$
- * drag crisis at $Re \approx 3 \times 10^5$: boundary layer undergoes transition from laminar to turbulent flow

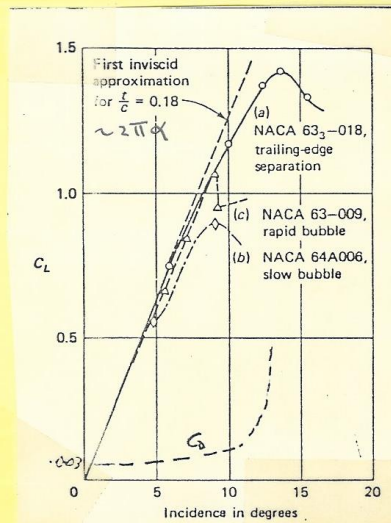
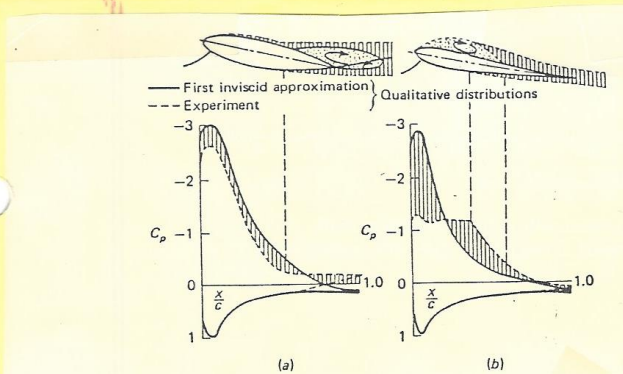
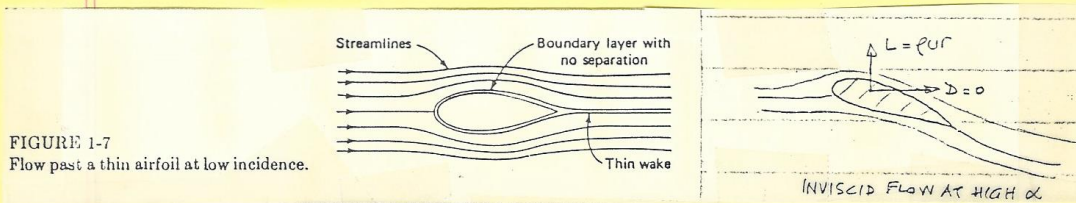




The flow is also affected by other parameters such as: pre-stream turbulence, roughness, & Mach number.

Although turbulent separated flow is quite commonly found in engineering applications, as we shall see through our discussions of various flows, they are the most difficult to predict. Thus, even the simple geometry of a circular cylinder presents great difficulties to the fluid mechanic.

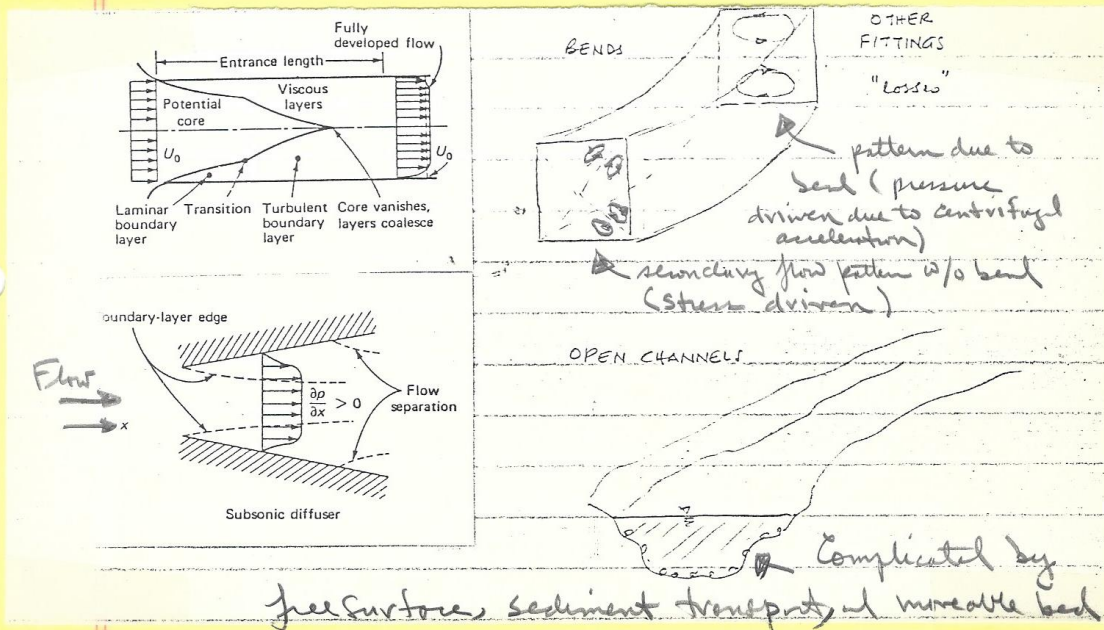
(S) The two-dimensional airfoil: Streamlined body



- * For large Re at small α , viscous effects are confined to thin boundary layer & narrow wake. Inviscid solution is a good approximation.
- * For increased α , viscous flow separates: rear TE for large t/c , and rear LE for small t/c
- * Separation leads to stall: loss in lift

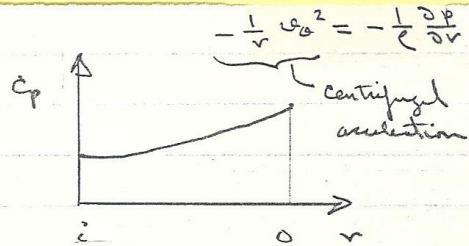
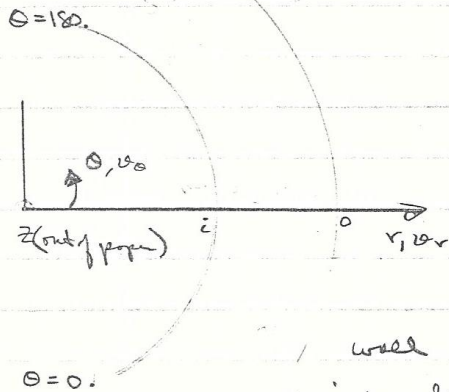
(c) Duct flow

Examples (a) & (b) are called external flows. Next, we consider an internal flow. Still yet another category of viscous flow is free-shear flow (wakes, jets, mixing layers)



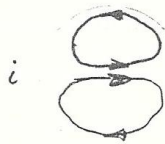
* Under most conditions, internal flows are dominated by viscous effects & the inviscid-flow solution does not represent a good approximation

2) Flow in a bend:



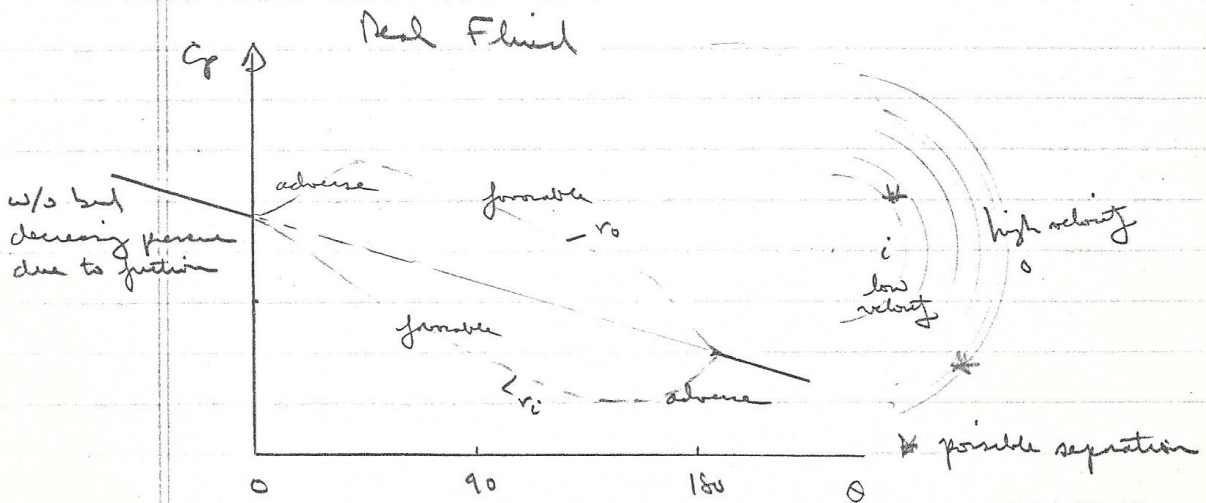
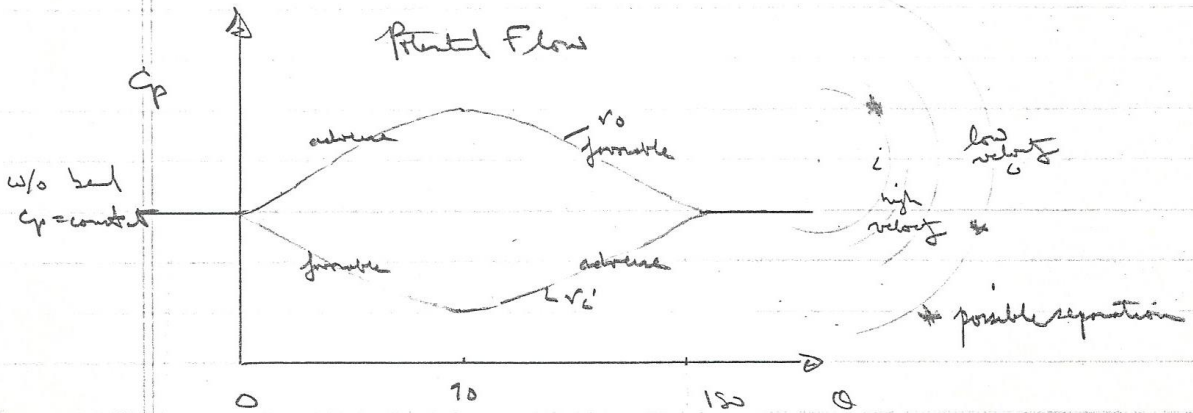
ie $\frac{dp}{dr} > 0$ which is an adverse pressure gradient in r direction. The

slower moving fluid near wall responds first at a swirling flow pattern results.



This swirling flow represents an energy loss which must be added to the h_L

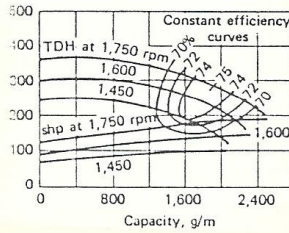
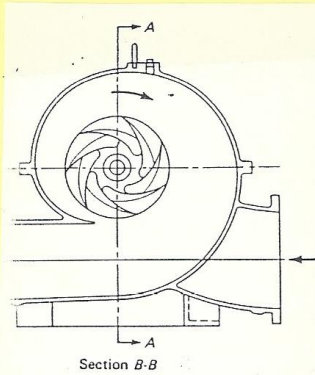
Also, flow separation can result due to adverse longitudinal pressure gradients which will result in additional losses



This shows potential flow not a good approximation in internal flows (except points near entrance)

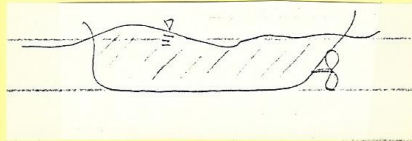
(d) Turbo machinery

- * geometry of flow is so complex that most of our knowledge is empirical
- * unsteady flow effects
- * cavitation



(e) ships

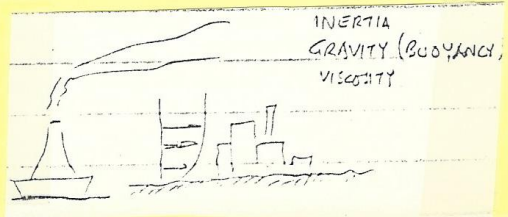
inertia, gravity, viscosity



(f) airplanes

inertia, viscosity, compressibility

(g) Ocean / Atmosphere



Some Important Effects of Viscosity

1. Transmission of Tangential Forces & Sliding Motion

Motion & no slip condition cause viscous shear stress, which diffuses into fluid (normal to direction of motion). Exploited by viscous pumps & film lubrication systems in dragging fluid from regions of low to high pressure.

2. Generation Vorticity

Vorticity is generated by viscous forces which are large near no-slip surfaces. There is a direct relationship between the viscous shear stress & vorticity.

$$\begin{aligned} \tau_x &= \mu n_y = -\mu \omega_z \\ \tau_{ij} n_j &= -\mu \omega_i n_i & \frac{D\omega}{Dt} &= \underbrace{(\omega \cdot \nabla) \omega}_{\text{vortex stretching}} + \underbrace{\nu \nabla^2 \omega}_{\text{diffusion}} \\ \tau_{ij} &= \mu \epsilon_{ij} \quad (\rho = \text{const.}) \end{aligned}$$

3. Inertia vs. Viscosity (convection vs diffusion)

$$\begin{aligned} \text{Inertia} &= \rho L^3 \omega^2 L = \rho L^2 \omega^2 & \text{Re} &= \frac{\text{inertia}}{\text{viscosity}} = \frac{\rho U L}{\mu} = \frac{U L}{\nu} \\ \text{Viscosity} &= \mu \frac{U}{L} \times L^2 = \mu U L \end{aligned}$$

Consider stirring coffee or honey

coffee: $\bar{U} = 1 \text{ cm/s}$, $D = 6 \text{ cm}$, $\nu = 4 \times 10^{-3} \text{ cm}^2/\text{s}$
 $Re = 1500$

honey: $Re = 1$

4 Drag & Propulsion

$$C_D = \frac{24}{Re} \quad \begin{matrix} 2/3 C_F \\ 1/3 C_p \end{matrix}$$

deformation
acceleration

Low Re : creeping motion

$$\nabla p \sim \mu \nabla^2 v$$

High Re : $C_D = C_F + C_p$

skin friction drag
form drag

proportion depends on body shape

5 Flow separation: ω , $\overline{u_i u_j}$, unsteady, etc.

6 Instability

Small perturbation leads large flow change.
 μ can damp or augment instability.

7. Dissipation of Mechanical Energy & Production Entropy

8. History vs. Immediate Effects

